Energy and Cost Analysis of an Integrated Photovoltaic and Heat Pump Domestic System Considering Heating and Cooling Demands

Mikel Arenas-Larrañaga [1,2,*] **, Maider Santos-Mugica** [1] **, Laura Alonso-Ojanguren** [1] **and Koldobika Martin-Escudero** [2]

1 TECNALIA, Basque Research and Technology Alliance (BRTA), Area Anardi 5, ES-20730 Azpeitia, Spain; maider.santos@tecnalia.com (M.S.-M.); laura.alonso@tecnalia.com (L.A.-O.)
2 ENEDI Research Group, Department of Energy Engineering, University of the Basque Country (UPV/EHU), Torres Quevedo 1, ES-48013 Bilbao, Spain; koldobika.martin@ehu.eus
* Correspondence: mikel.arenas@tecnalia.com

Abstract: The integration of photovoltaic panels and heat pumps in domestic environments is a topic that has been studied extensively. Due to their electrical nature and the presence of elements that add thermal inertia to the system (water tanks and the building itself), the functioning of compression heat pumps can be manipulated to try to fulfill a certain objective. In this paper, following a rule-based control concept that has been identified in commercial solutions and whose objective is to improve the self-consumption of the system by actively modulating the heat pump compressor, a parametric analysis is presented. By making use of a lab-tested model, the performance of the implemented control algorithm is analyzed. The main objective of this analysis is to identify and quantify the effects of the main parameters in the performance of the system, namely the climate (conditioning both heating and cooling demands), the photovoltaic installation size, the thermal insulation of the building and the control activation criteria. A total of 168 yearly simulations have been carried out. The results show that the average improvement in self-consumption is around 13%, while the cost is reduced by 2.5%. On the other hand, the heat from the heat pump and the power consumed increase by 3.7% and 5.2%, respectively. Finally, a linear equation to estimate the performance of the controller is proposed.

Keywords: heat pump; photovoltaic panels; Dymola; Modelica; self-consumption

1. Introduction

Due to the need to raise the share of renewables in all sectors and the decarbonization of society, air-source domestic heat pumps have been identified as being cleaner and more efficient alternatives to traditional gas boilers. In Europe, 2.17 million heat pumps were sold in 2021, 34% more than the previous year, according to [1].

In parallel, domestic photovoltaic (PV) installations for self-consumption have also spread [2]. Because of the variable and weather-dependent nature of photovoltaic power, electric batteries have been inserted to boost the self-consumption of households with PV installations. Thus, energy that is not instantly consumed in the house is stored in batteries for later consumption, e.g., when power from the panels is not available. This reduces dependence on both the grid and the renewable generation source (usually non-controllable and variable). Additionally, due to the price difference between buying and selling energy from the grid, it could make sense to increase self-consumption while reducing the energy that is sold to the grid.

Storing the excess as thermal energy is another way to improve the self-consumption of the system. Provided that a heat pump-based thermal installation is already present, no

extra elements have to be added; the water tanks and the thermal inertia of the building can be used actively [3].

Some heat pump manufacturers have started implementing some solutions in their commercial products to boost the self-consumption of the whole system [4–6].

The question of controlling and optimizing the integration between heat pumps and PV panels has been quite extensively analyzed in the literature [3,7–14]. The studies can be grouped into two different solutions: rule-based controls and optimization-based controls. The former are strategies based on pre-determined, relatively simple rules and work only with instantaneous information. Optimization-based strategies work on optimization algorithms that try to minimize or maximize a certain variable in a prediction horizon. Generally, when speaking about this kind of controls, Model Predictive Controls (MPC) are considered; that is, algorithms that are able to predict the performance of the system by making use of a model of it. In [3], more simplistic ON–OFF controls are also analyzed, while different levels of prediction can be added, as shown in [15].

A comparison of the performance of five different control approaches for the integration of air-source heat pumps and PV panels is carried out in [14]: four rule-based controllers and a convex MPC approach. The climate from Potsdam (Germany) was used and only heating demand was considered. Four different storage volumes were introduced. It was concluded that MPC outperforms the rest of the approaches. The cost of electricity was reduced by 2–4% for rule-based controls; while for the MPC approach, it was reduced by 6–16%.

In [12], four complexity levels of a rule-based controller were analyzed for five Italian climates and two insulation levels. Both cooling and heating were considered. In this case, the rule-based control was based on a pre-defined equation that gives the optimum modulation of the heat pump to consume the excess electricity. The pre-defined equation is only valid for the specific heat pump. The study focused on grid consumption and self-consumption, claiming that they decreased by 17% and increased by 22%, respectively, for the case of Bolzano. In addition, it was claimed that the lowest energy reduction levels were obtained for Milan and Trento because of their low-solar radiation and low-temperature levels.

An analysis of the boundary conditions of a rule-based controller is presented in [13]. They consider six European locations and cooling needs are neglected, despite having climates with supposedly considerable cooling demands, as in Rome or Madrid. They concluded that large monetary savings were possible for both Spain and Germany.

Despite being a subject that has received attention in terms of investigation, considering the identified works, the real effect of the rule-based self-consumption booster controllers in terms of, not only cost savings, but also in the potential rise of consumed power, is as yet unclear. Considering both heating and cooling demands is seen as essential as well, since climate change will increase the latter. Even though heat pumps have traditionally been seen as equipment for heat production, they also have the potential to cool spaces, a capacity that should not be neglected due to the rising temperature all over the globe. As stated previously, ref. [12] is one of the few studies that considers these cooling demands.

The main objective of this study is to analyze, via simulation, the effect of a rule-based self-consumption booster, by making use of a previously lab-tested model. The controller is inspired by those implemented in commercial solutions, such as in [4–6]. To do so, a parametric analysis has been carried out with different climates, while also changing the key parameters that define the behavior of the controller.

The effects of the main parameters on the performance of the system are identified and quantified through a regression analysis. As a result, a linear equation that can be used to estimate the performance of the controller is obtained.

2. Methodology

In order to carry out the parametric analysis, different hypothetical scenarios were simulated. The objective of these scenarios was to try to represent the different conditions under which the rule-based controller could work. Thus, seven European climates were used: four within Spain (some with notorious cooling demands) and three from other parts

of Europe. Alongside the climates, two different insulation levels, three different PV sizes and three different minimum excess values for the activation of the excess mode were used for the discussion. All the mentioned parameters are introduced first in Section 3.

The whole study is based on the comparison between the so-called base case scenario (there is no integration between the PV and the heat pump) and the scenario in which the rule-based controller is enabled.

2.1. Inputs

The following climates were chosen: Albacete (Spain, semi-arid), Barcelona (Spain, subtropical), Berlin (Germany, oceanic with continental influence), Bilbao (Spain, oceanic), Cordoba (Spain, Mediterranean), Paris (France, oceanic) and Stockholm (Sweden, continental). Their location can be seen in Figure 1.

Figure 1. Location of the selected cities.

Apart from the location (7 European cities), two insulation levels, three PV sizes (2.75 kW, 3.85 kW and 4.95 kW), and three minimum excess values (1400 W, 1600 W and 1800 W) were included in the analysis.

2.2. KPI's

When it comes to the Key Performance Indicators (KPI), the following variables were analyzed:

- The self-consumption ratio (SCR) (-): defined as the ratio between the energy coming from the PV panels that is locally consumed and the total amount of PV generation.
- Cost (EUR): defined as the amount of money that the consumer has to pay for the energy term of the heat pump.
- Specific cost (EUR/kWh): defined as the amount of money that the consumer has to pay per kilowatt-hour of provided heat.
- Produced thermal energy (kWh): total amount of heat and cool produced by the heat pump.
- Consumed power (kWh): total amount of power consumed by the heat pump.

3. System Modeling

The system used for the parametric analysis consists of a detached house of two floors with a total area of 140 m^2 and four inhabitants. The building is oriented to the four cardinal directions, and it has a radiant floor for heat distribution purposes.

The heating and cooling system of the household can be seen in Figure 2. The heat is produced by a propane-based 12 kW air-source heat pump. Two water tanks are used in the installation. One of them has a volume of 80 L and is used as a buffer for climatization. The other has a capacity of 200 L and is used for storing DHW (Domestic Hot Water). Both tanks are part of a single hydraulic module. Nevertheless, in terms of performance, they work as completely separate components.
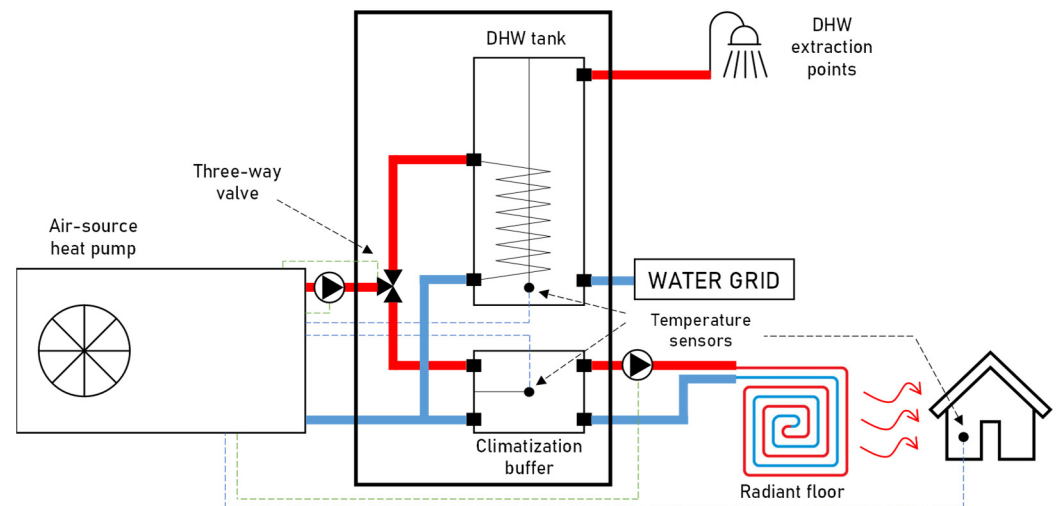

Figure 2. Scheme of the domestic heating and cooling system. The red lines represent tubes carrying hot water; the blue lines represent tubes carrying water at a lower temperature; the dashed blues lines represent sensor readings; the dashed green lines represent control signals sent to the actuators.

The volumes of the tanks are considered standard for the application being analyzed in this document: a household inhabited by four persons and a radiant floor system of a medium-sized detached house. This decision is validated with a manufacturer with extensive experience in the sector [16].

The control implemented for the integration of the PV panels and the heat pump is a rule-based control (an algorithm that only considers instantaneous information and works by following relatively simple yes–no conditions) whose main objective is to boost the self-consumption ratio while modulating the compressor speed to reduce the electricity excess that is introduced to the electricity grid.

The system model is elaborated with the open-source *Buildings* library in Dymola [17]. This Modelica-based library is believed to be adequate for the exercise that is proposed in this article due to its multiple flexible and fast-to-implement models for building-level simulations.

3.1. Demands

The household has two sources for thermal demand: climatization (heating and cooling) and production of DHW. The modeling decisions for each of them are presented in the following sections.

3.2. Building

Two scenarios have been defined regarding the building insulation: a well-insulated new household (NHH) and a more poorly insulated older household (OHH). For the well-insulated house, the Spanish Building Technical Code (CTE in its Spanish denomination) is used to size the necessary insulation [18]. For the second house, half of the insulation is supposed to represent older or refurbished buildings.

The model also considers the radiation effect through windows, and its effect on walls and roof. A ventilation rate of 73 L/min is considered following the CTE [18]. The internal temperature of the house is considered uniform.

In Table 1, the heating and cooling demands for each climate and building are shown.

**Table 1.** Heating and cooling demands for each location.

	Heating Demand (kWh·m^{-2})		Cooling Demand (kWh·m^{-2})	
	NHH	**OHH**	**NHH**	**OHH**
Albacete	26.20	50.98	32.27	26.50
Barcelona	19.26	36.23	32.04	26.83
Berlin	53.19	92.69	10.76	5.41
Bilbao	25.01	47.40	13.55	6.10
Cordoba	15.88	26.88	49.56	54.41
Paris	42.86	75.67	12.91	6.92
Stockholm	71.58	123.55	4.98	0.87

3.3. DHW

The DHW demand profile is based on the norm UNE-EN 16147:2017 [19]. The M profile from Annex A is selected since it is the one closest to the CTE requirements [18]. The standard proposes a demand of 5.845 kWh·day^{-1} while the CTE fixes a demand of 28 L·day^{-1}·person^{-1}, which, translated to energy, is 6.14 kWh·day^{-1}. The energy extractions according to the M profile in UNE-EN 16147:2017 are shown in Figure 3.
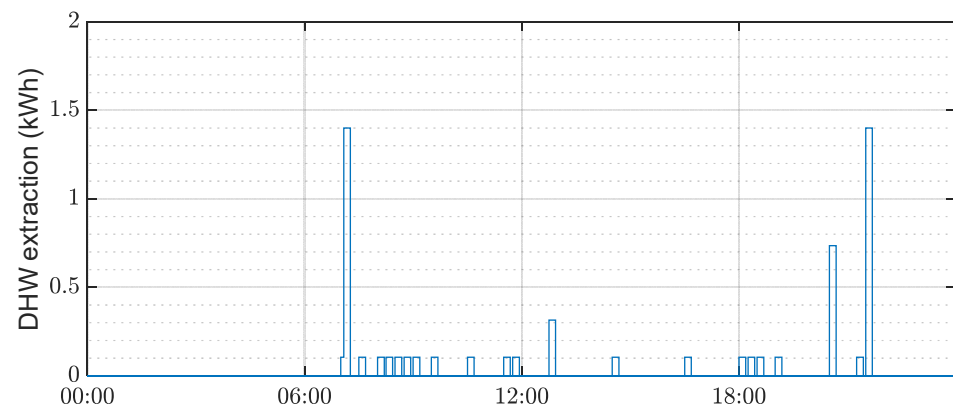
Figure 3. DHW extractions in UNE-EN 16147:2017, Annex A, M profile.

Based on the profile proposed by the norm, the energy extractions have been normally distributed, in both amplitude and time, around the values that are present in the norm, in order to obtain more realistic behaviors. Therefore, all the days have different energy extraction profiles. An example of the energy extractions of a specific day is shown in Figure 4.

Apr 10, 2020
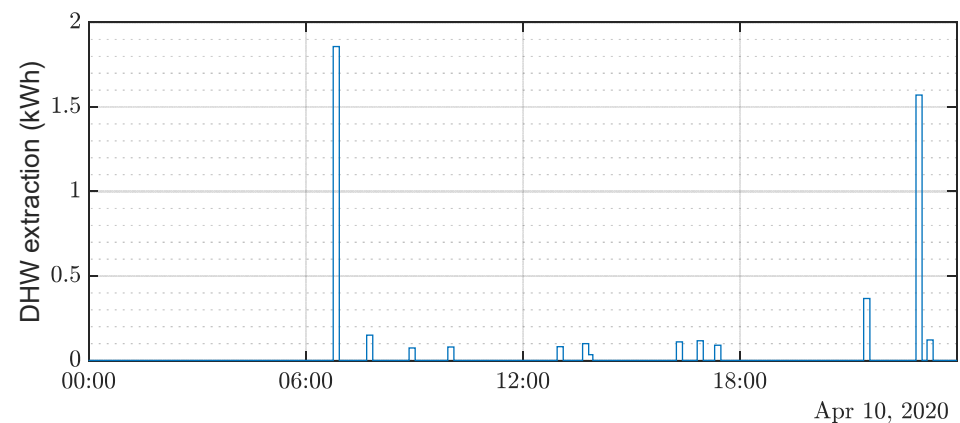
Figure 4. DHW extractions on 10 April.

3.4. Electrical Load

The consumption of the rest of the electrical appliances of the household (washing machine, dishwasher, electronic devices, etc.) is modeled by making use of the CREST model, explained in detail in [20]. This high-resolution thermal-electrical demand model is based on a bottom-up structure that uses stochastic programming techniques applied to real-world data collected in the UK. Electrical heating has been removed from the list of appliances since it is not present in the analyzed system.

3.5. Thermal System

The thermal system of the household is based on a propane air-source heat pump, with two tanks and radiant floor for heating and cooling distribution.

3.6. Heat Pump

The dynamic model of the heat pump is derived from the compressor curves and calibrated with laboratory tests. The heat pump has a modulating compressor. That is, it is able to work under different rotating speeds by making use of an inverter. The faster the running speed (also referenced as frequency in the document), the more energy it will consume.

A photo of the main components used in the laboratory tests is shown in Figure 5, provided by [16]. The heat pump is in the foreground. It uses propane (R290) as the refrigerant and can reach temperatures up to 70 °C. Under nominal conditions (air at 7 °C and input water at 30 °C), it supplies 12 kW with a Coefficient of Performance (COP) of 4.7. In the background, on the left-hand side, the hydraulic module that combines both the DHW tank and the climatization buffer can be seen. Both components are connected by insulated tubes.

Figure 5. The laboratory setting.

The heat pump is modeled by means of performance maps (a group of equations that correlate the most important output variables of the machine with the main inputs). The inputs of these second-degree polynomials (Equations (1) and (2)) are the inlet air and water temperature ($T_{air,in}$ and $T_{water,in}$, respectively), the compressor running speed (n_{comp}) and the working mode (w) (heating or cooling). The outputs are the compressor power consumption ($\dot{P}_{comp}$) and the provided heat or cold capacity ($\dot{Q}_{inner}$) in the inner heat exchanger. The concept is shown in Figure 6.

$$\dot{Q}_{inner} = f\left(T_{air,in}, T_{water,in}, n_{comp}, w\right) \tag{1}$$

$$\dot{P}_{comp} = g\left(T_{air,in}, T_{water,in}, n_{comp}, w\right) \tag{2}$$
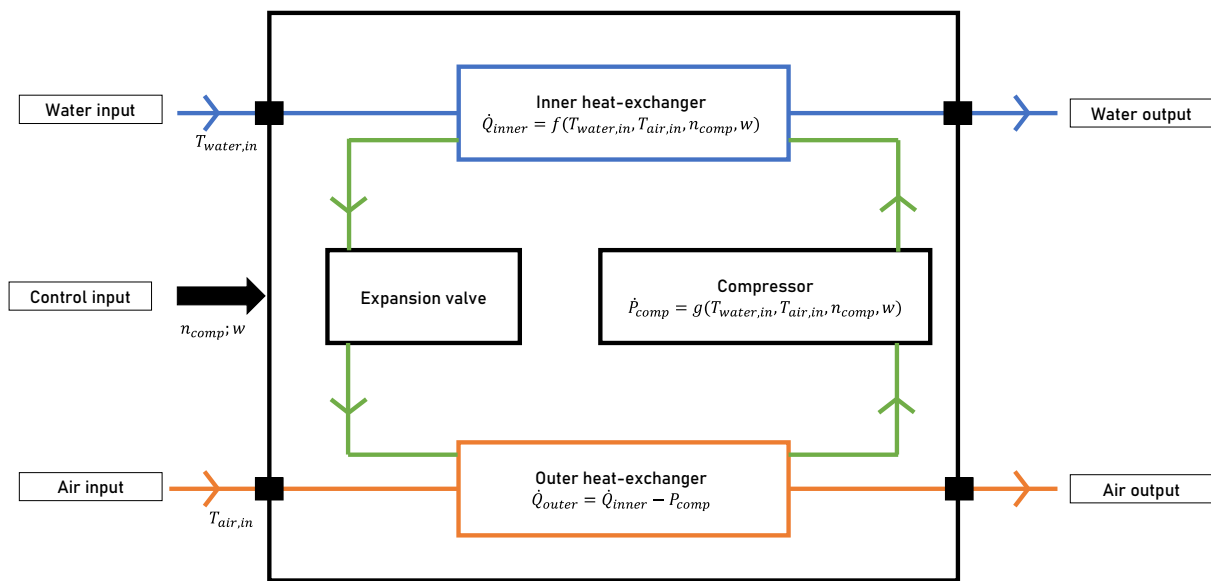
Figure 6. Concept of the performance maps used for modeling the heat pump. The blue line represents the stream of water; the orange line represents the stream of air; the green line represents the stream of refrigerant.

The dynamics of the heat pump are modeled with lumped volumes in the heat exchangers.

Figure 7 shows the performance of the model (orange) when compared to the lab tests (blue). As can be observed, the model is able to capture both the provided heat and the consumed power. Excluding the very short peaks that are observed in the transients, the error is always below 10%. Thus, the model is thought to be precise enough for the analysis of this document.


(**a**) Heat provided by the heat pump.

(**b**) Power consumed by the heat pump.
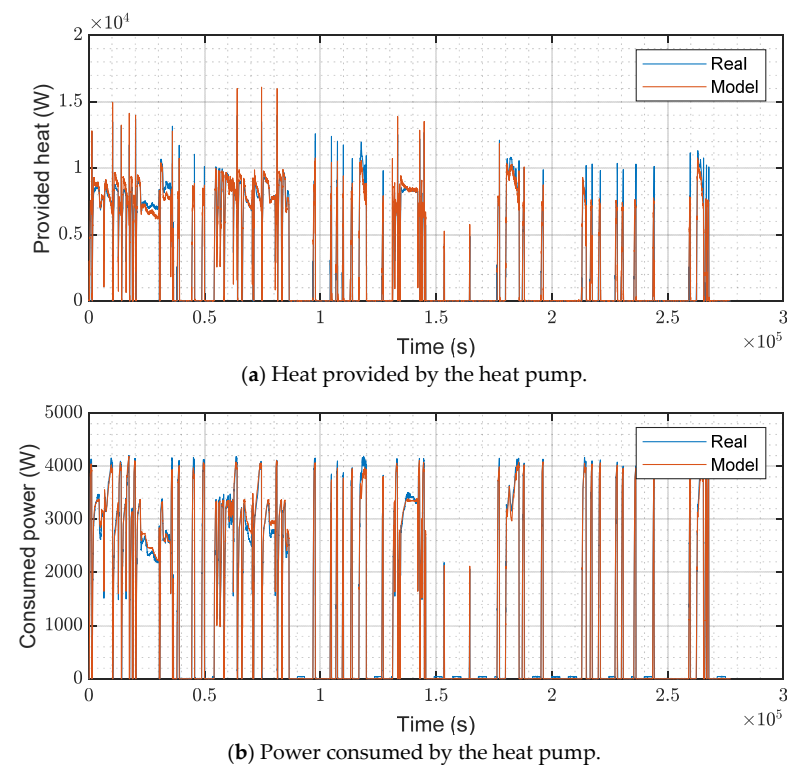
Figure 7. Comparison of the experimental data (blue) and the results of the heat pump model (orange) for (**a**) the provided heat and (**b**) the consumed power.

3.7. Heat Storage

The models for the two water tanks consider stratification. The heat exchange between the internal coil and the water for the case of the DHW tank is also considered. The specific parameters of each tank have been calibrated by making use of experiments.

Figures 8 and 9 show the performance of the model (orange) when compared to the lab tests (blue). For the climatization buffer, two sensors are inserted at different heights. For the DHW tank, three sensors are used to measure the temperature. As with the heat pump, the models for both the climatization buffer and the DHW tank are thought to be valid for the purpose of this document. In the climatization buffer, and excluding the transients, the maximum absolute error is 1.5 K. In the DHW tank, there are bigger differences; nevertheless, the original model is improved after the calibration process and is able to capture the overall performance of the tank.
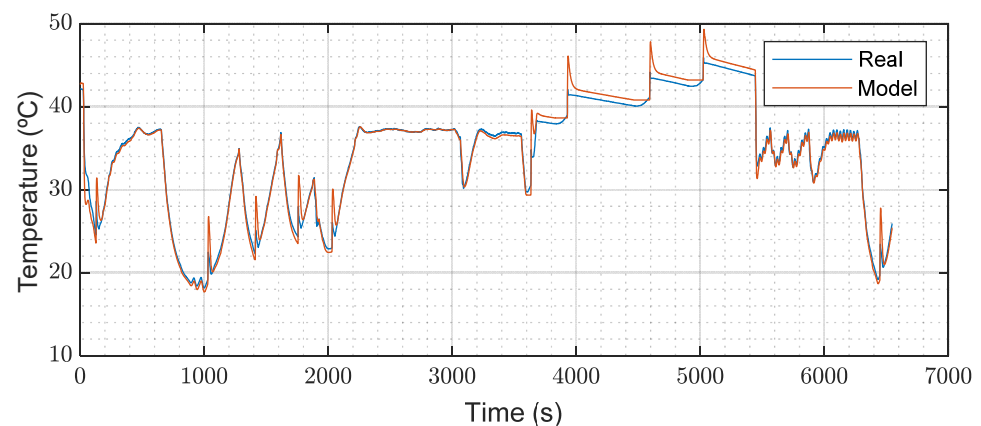
(**a**) Top temperature.
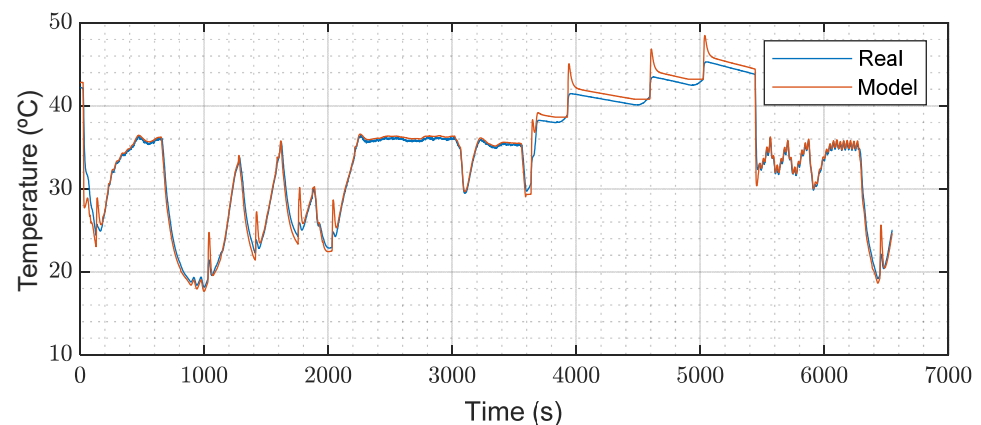
(**b**) Bottom temperature.

Figure 8. Comparison of the experimental data and the results of the climatization buffer model for (**a**) the top temperature and (**b**) the bottom temperature.
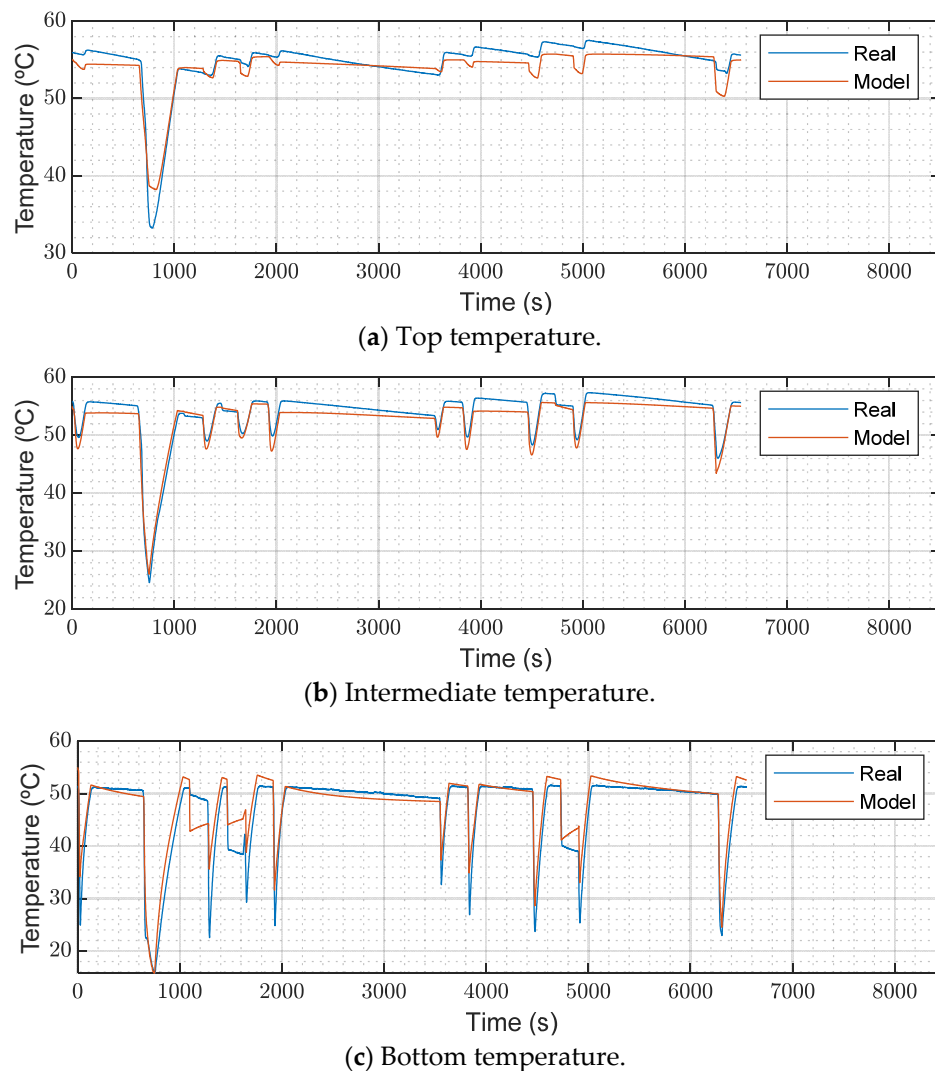
(a) Top temperature.

(b) Intermediate temperature.

(c) Bottom temperature.

Figure 9. Comparison of the experimental data and the results of the DHW tank model for (**a**) the top temperature, (**b**) the intermediate temperature and (**c**) the bottom temperature.

3.8. Heat Distribution

Radiant floor is used to distribute the heat and cold produced by the heat pump and stored in the water tanks. A single water circuit goes through both floors heating up the building. The implemented model uses the NTU method for the heat transfer between the pipe and the floor material.

3.9. PV Installation

Three discrete PV installations are used for the parametric analysis: 2.75 kW, 3.85 kW and 4.95 kW of peak power. It is supposed that they always work at the MPP (Maximum Power Point). The thermal model explained in [21] is also introduced to consider the effect of the temperature of the panels.

3.10. Other Aspects

For economic calculations, electricity prices for the Spanish market are considered [22].

A simulation time step of 10 s is used to try to replicate the quick changes in compressor speed and the small DHW extractions.

3.11. Implemented Control

The system is controlled in MATLAB-Simulink by importing the model elaborated in Dymola via the Functional Mock-up Interface (FMI). In this chapter, the standard control that rules the heat pump and the thermal system are explained. Then, the rule-based control that aims to boost the self-consumption is introduced.

3.12. Standard Control

The standard control is designed to maintain the comfort temperature in the building, the DHW tank and the climatization buffer. The set-points for cooling and DHW are constant; whereas for heating, a heating curve is inserted to control the temperature of the buffer. The heating curve is shown in Figure 10, while the rest of the values are shown in Table 2. To avoid a constant ON–OFF performance, the upper and lower hysteresis values are inserted as well.
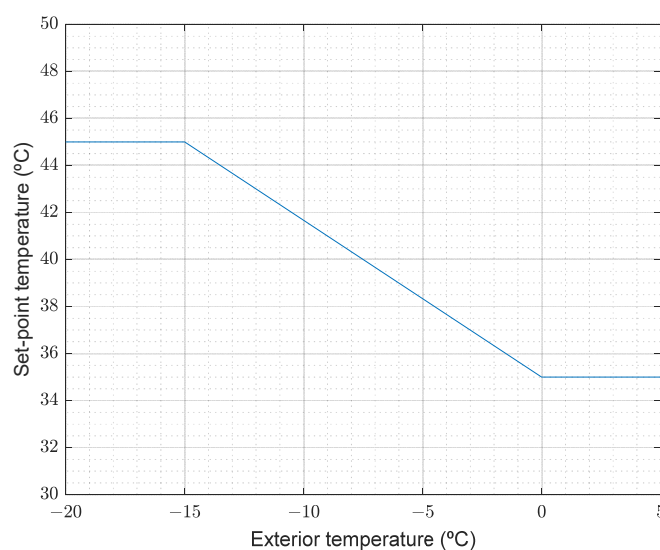

Figure 10. Heating curve for climatization buffer set-point.

Table 2. Standard temperature set-points.

	Set Point (°C)	Upper Hysteresis (°C)	Lower Hysteresis (°C)
Climatization buffer in heating mode	Heating curve	Heating curve + 2	Heating curve − 2
Climatization buffer in cooling mode	12	14	10
DHW tank	50	50	48

The control prioritizes the DHW over the climatization, meaning that the heat pump will always heat up the DHW tank, irrespective of whether there is a climatization demand [23]. When working in DHW mode, the compressor always works at maximum power to try to compensate for the fast hot water extractions from the tank. When working in climatization mode, the compressor is activated at maximum power, but it starts to regulate itself after getting closer to the set-point.

When it comes to the control of the building temperature, the set-points have also been obtained from the CTE requirements [18], with different temperatures for heating and cooling seasons, as well as daytime and night-time, as shown in Table 3.

Table 3. Interior temperature set-points.

	Daytime	Night-Time
Heating season	20 °C	17 °C
Cooling season	25 °C	27 °C

3.13. Rule-Based Self-Consumption Booster

The control for the integration of the PV panels and the air-source heat pump are inspired by the algorithms that can be found in the literature and which some manufacturers have started to implement in their products.

It basically considers whether the measured PV excess or surplus that is being introduced into the electrical grid is above a defined value for a certain amount of time. If that condition is met and there is no demand for DHW and/or climatization (that is, the temperatures are above the set-points), the controller starts working in a separate mode, the so-called *excess mode*.

While working in this mode, the set-points of the tanks change to more demanding values. For DHW, the new set-point is 60 °C (a value which is higher than the standard set-point, but not excessively so, and consciously lower than the maximum operating temperature of a propane air-source heat pump of around 70 °C). For space heating, five degrees are added to the heating curve shown in Figure 10; while the space cooling set-point is maintained in order to avoid water condensing problems on the floor. Similarly, the set-points of indoor air are either increased or reduced. In the heating season, the set-point is increased by 2.5 K; while in cooling season, it is reduced by 2.5 K.

When the excess is negative for one minute (a discrete value that could be changed in the final real-world application) or there is a DHW or climatization demand, the system goes back to normal functioning. This concept is shown in Figure 11.
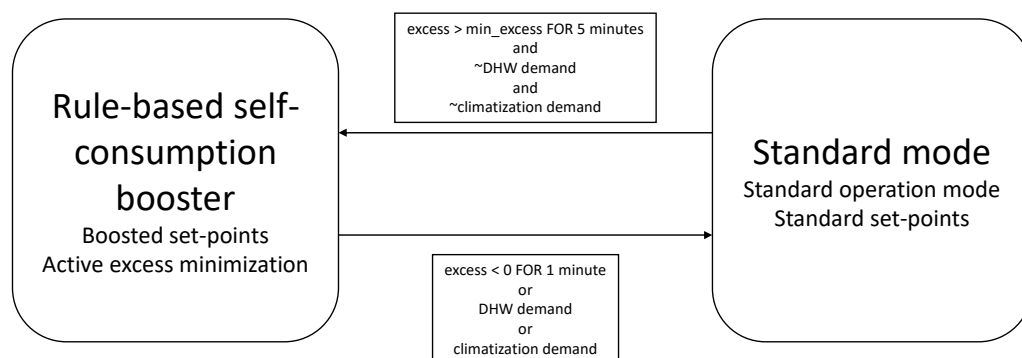

Figure 11. Concept of the rule-based self-consumption booster controller with its activation and deactivation conditions.

The same concept is reflected in the following pseudocode:
if standard_mode AND (excess > min_excess for 5 min) AND NOT(demand) **then**
excess_mode
elseif excess_mode AND [(excess < 0 for 1 min) OR demand] **then**
standard_mode
end

When working in the excess mode, the heat pump modulates the compressor's frequency to minimize the PV surplus. Generally speaking, when there is enough PV surplus, the modulating frequency of the compressor is raised. Thus, the heat pump consumes more power and the surplus decreases. If the surplus is low (close to 0), it is supposed that the system could start consuming power from the electric grid, which is not desirable, since it will consume power to fulfill some set-points that are not the ones defined in the standard mode. Consequently, the modulating frequency of the compressor is reduced; by doing so, the PV surplus enters a safer zone.

Specifically, starting from a low modulation, the frequency is raised by 2 Hz if the surplus is higher than 150 W for 10 s; if the surplus is lower than 50 W for 10 s, the frequency is reduced by 2 Hz; if neither of these happen, the frequency value does not change.

Its corresponding pseudocode would be as follows:

if excess > 150 W for 10 s **then**

$\qquad n_{comp} = n_{comp} + 2$ Hz

elseif excess < 50 W for 10 s **then**

$\qquad n_{comp} = n_{comp} - 2$ Hz

else

$\qquad n_{comp} = n_{comp}$

end

## 4. Results

After simulation of 168 cases (42 for the base scenario and 126 for the controlled scenario), the obtained results are presented in this section.

4.1. Functioning of the Rule-Based Control

In order to visualize the functioning of the rule-based scenario, Figure 12 shows the performance of the temperatures when the excess mode is activated. As can be seen, the excess mode is activated at around 13:10. First the DHW tank is heated up to 60 °C, the boosted set-point for that tank. After reaching that temperature, the climatization buffer is heated up to 45 °C. Later on, the building itself starts to work as a heat storage unit.
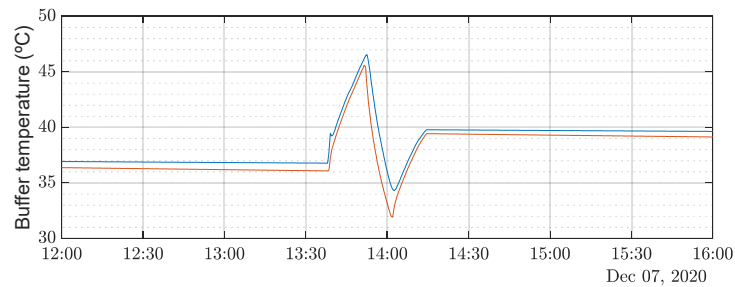
(**a**) Temperature at the climatization buffer. The two lines represent the temperatures at the upper and bottom part of the buffer.
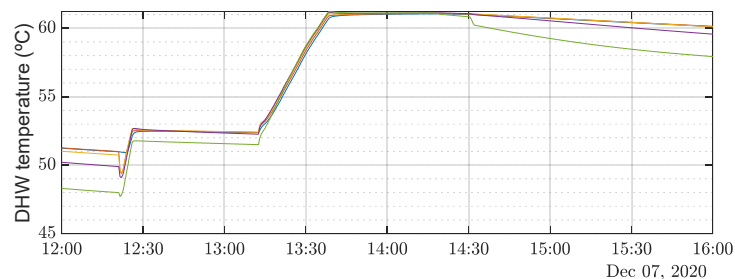

(**b**) Temperature at the DHW tank. The lines represent the temperatures at different levels in the tank.
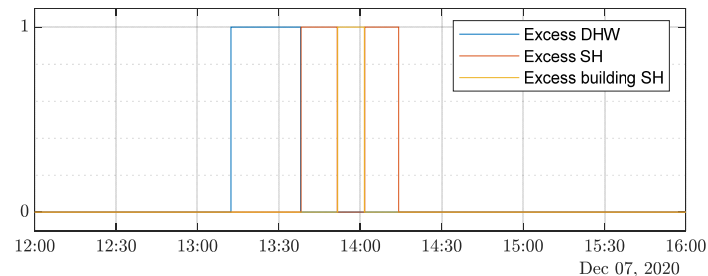
(**c**) Activation of the sub-modes within the excess mode.

Figure 12. Performance of the temperatures on a day in which the excess mode is activated. Temperatures at the climatization buffer and the DHW tank are shown in (**a**) and (**b**) respectively. In (**c**), the activations of the sub-modes within the excess mode can be seen.

Figure 13 shows the modulation of the compressor frequency, alongside the surplus power that is bought or sold in the grid. Thanks to the implemented control, the positive excess is minimized by making use of the power modulation capacity of the heat pump.
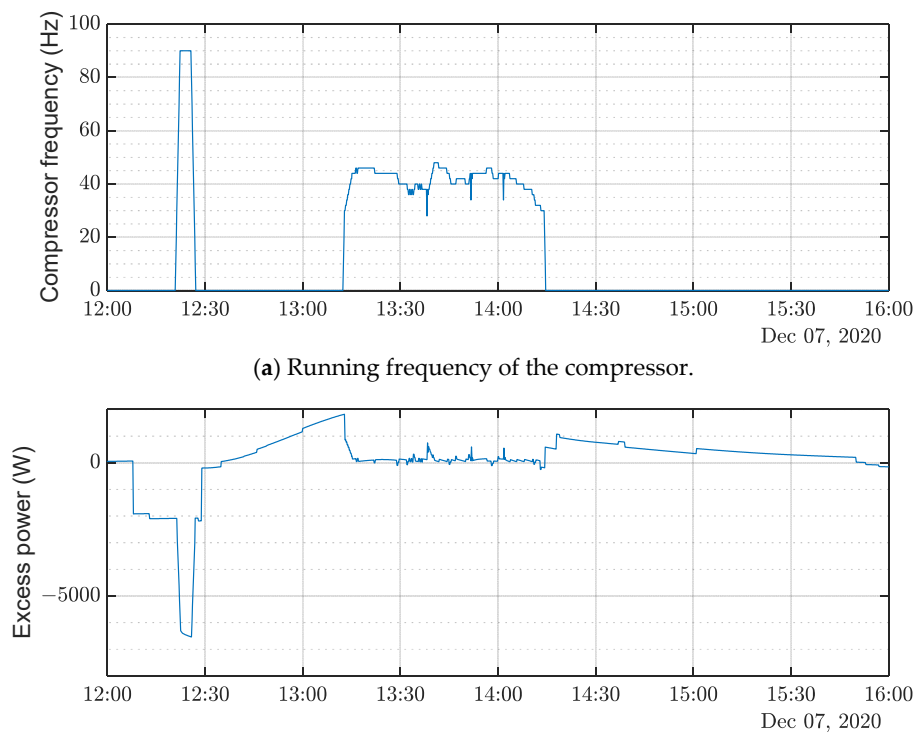
(**a**) Running frequency of the compressor.

(**b**) The excess power injected (positive sign) or extracted (negative sign) from the electric grid.

Figure 13. (**a**) Compressor modulation under the excess mode and (**b**) the excess power on 7 December.

Due to the activation of the excess mode, the normal consumption pattern of the heat pump is modified. That is, when there is no control integration between the heat pump and the PV panels, the former is turned on whenever there is a demand; the power that is being generated by the PV panels is not considered as a parameter for decision-making purposes. Nevertheless, when the self-consumption booster is enabled, the power consumption of the HP is shifted to the central hours of the day, when the PV generation is higher, and thus there is a higher chance of electricity excess.

Figure 14 shows how the hourly energy flows are distributed throughout a year in NHH in Albacete for the controlled scenario.

In Figures 15 and 16, comparisons for the heat pump consumption and the energy coming from the electric grid, respectively, are pictured. The blue lines represent the base case scenario and the orange lines represent the controller case. Figure 15 shows how the consumption of the heat pump is shifted to the central hours of the day: from 10:00 to 14:00 the consumption of the heat pump is larger when compared to the base scenario; whereas, for the rest of the hours, it is smaller. On the other hand, Figure 16 shows how the energy inserted in the electric grid is reduced during the same hours: the energy that is consumed by the heat pump.
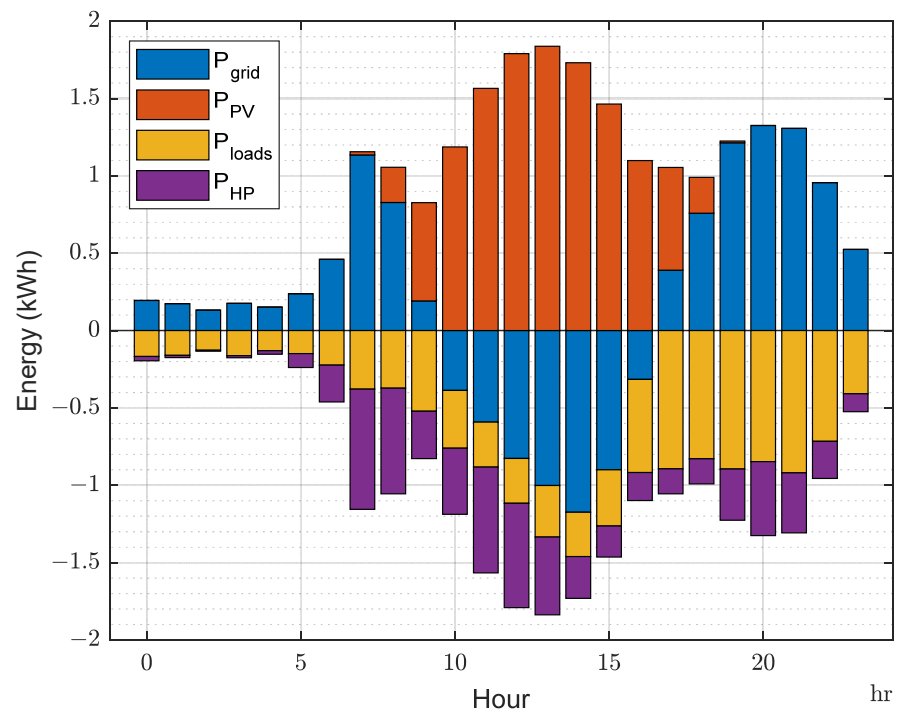
Figure 14. Hourly distribution of daily energy throughout a year in the controlled scenario.
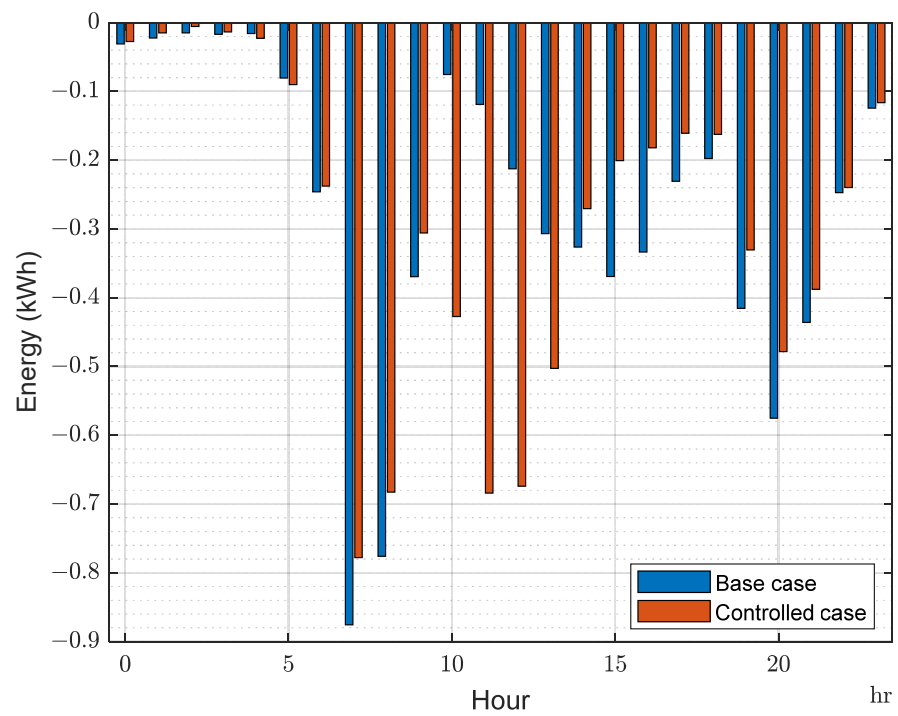

Figure 15. Comparison of hourly heat pump consumption throughout a year for the base and the controlled scenarios.
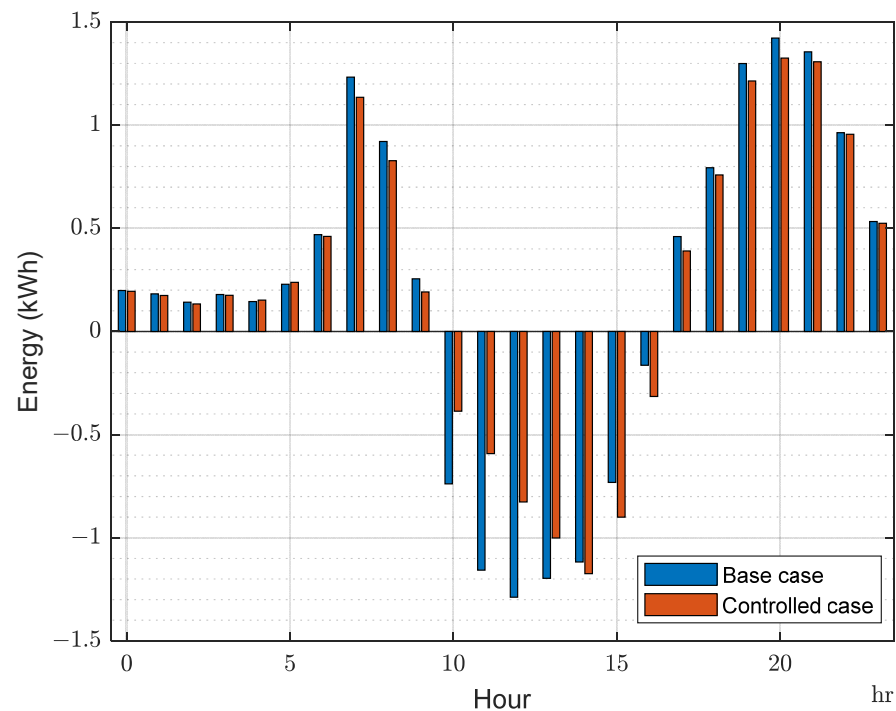
Figure 16. Comparison of the hourly consumed energy (positive values) or the inserted energy (negative values) in the electric grid throughout a year for the base and the controlled scenarios.

4.2. Parametric Analysis

The performance of the KPIs defined in the corresponding section is described in the following section. The so-called violin-plots have been used to capture the distribution of these parameters. This kind of graph adds another dimension that involves the frequency of the values: the more values there are in that area, the wider the graph is. For this parametric analysis, the violin-plot is divided into two halves: the left one captures the base case scenario and the right one captures the scenario in which the controller is enabled. Quartiles (colored areas) and mean values (crosses) are also represented.

It is necessary to consider that the main objective of the implemented rule-based control is to increase the self-consumption of the system. Thus, the mean self-consumption ratio is improved in every climate. The improvements are all between 9.7% (Cordoba) and 15.3% (Berlin), as can be seen in Figure 17.

By analyzing the effect independently and starting with the building insulation, OHH obtains slightly better self-consumption ratios. This can be explained by the fact that, in buildings where the heating demands are higher, it is easier to find days in which the indoor temperature has room to be boosted during the central part of the day, when the PV production is higher. Thus, the electrical power coming from the PV panels is consumed by the heat pump, increasing the self-consumption ratio, as shown in Table 4.
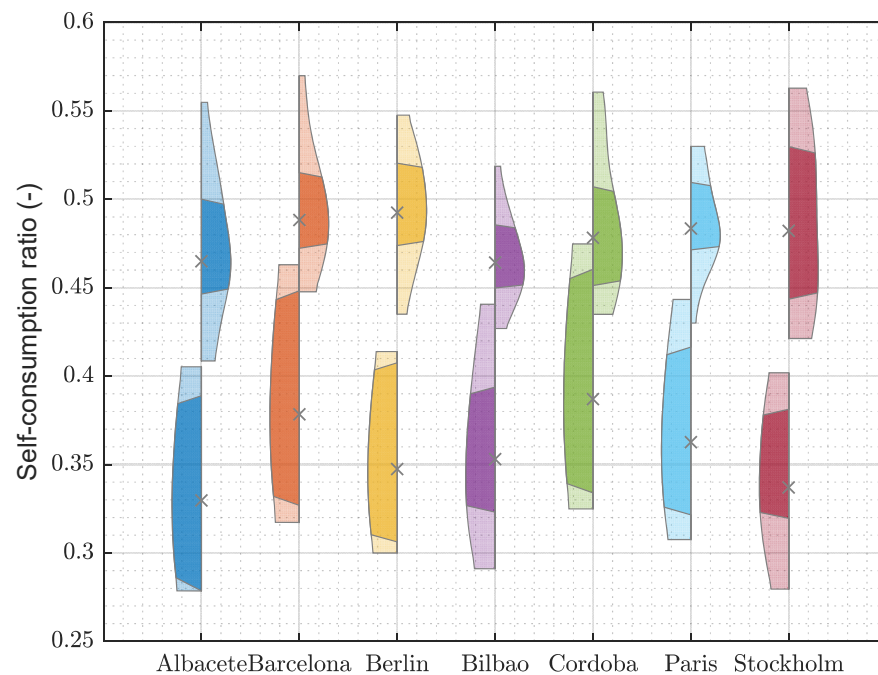
Figure 17. Self-consumption ratios for base case and controlled scenarios for every climate.

Table 4. Self-consumption values for base case and controlled scenarios for all climates and both insulation levels.

	NHH			OHH		
	Base	**Controlled**	**Improvement**	**Base**	**Controlled**	**Improvement**
Albacete	0.3346	0.4477	0.1131	0.3247	0.4855	0.1608
Barcelona	0.3868	0.4850	0.0982	0.3699	0.4932	0.1233
Berlin	0.3465	0.4745	0.128	0.3483	0.5120	0.1637
Bilbao	0.3735	0.4623	0.0888	0.3326	0.4661	0.1335
Cordoba	0.3944	0.4739	0.0795	0.3796	0.4861	0.1065
Paris	0.3741	0.4827	0.1086	0.3511	0.4981	0.147
Stockholm	0.3207	0.4456	0.1249	0.3532	0.5268	0.1736

Regarding the minimum excess value and the installed PV power, the effect is more evident. In Figure 18, the improvements in self-consumption in Berlin for NHH are shown. First, it can be seen that the higher the minimum PV excess, the lower the self-consumption improvement is. This effect is derived from the non-self-consumed power as the activation criteria become stricter. In other words, if the minimum excess value is 1800 W instead of 1400 W, the rule-based controller is enabled for a shorter amount of time, which decreases the self-consumption of the system.
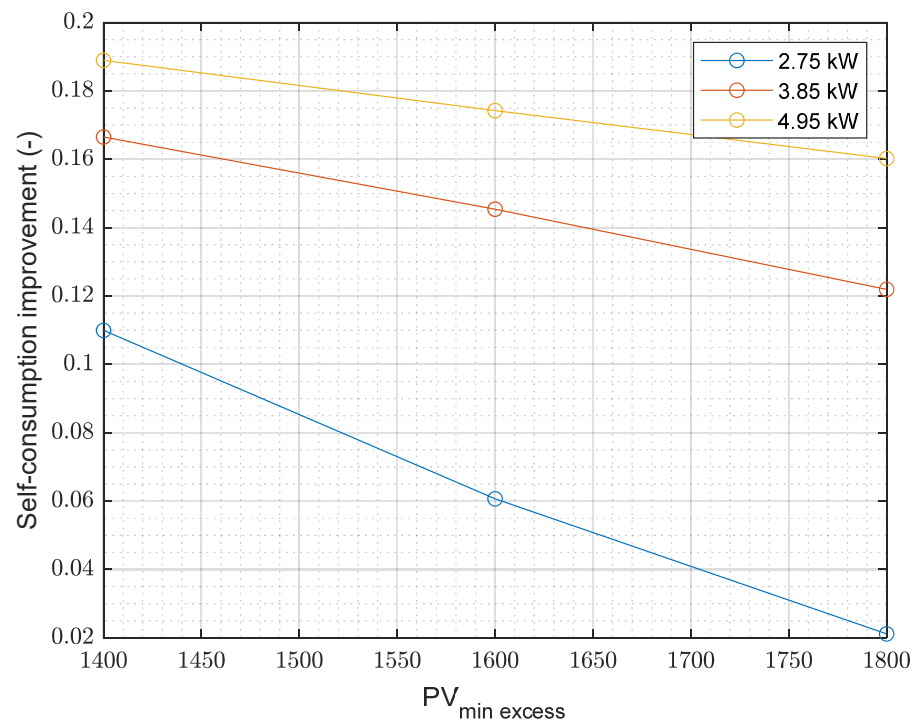
Figure 18. Parametric graph of the self-consumption improvement in Berlin for the NHH.

Furthermore, concerning the PV power installed in the building, greater improvements are achieved with larger PV installations. This is mainly due to the low-base scenario self-consumption ratios. Since the PV generation and the heat pump consumption are independent, large PV installations obtain worse self-consumption ratios if no control is implemented. When a certain control is inserted, a larger percentage of improvements are obtained.

Furthermore, the higher the PV installation, the smaller the effect of the minimum excess value. If the PV installation is large, the percentage difference between two certain minimum excess values becomes smaller, and therefore, so does the improvement in the self-consumption ratio.

The effect seen for the self-consumption ratio can also be observed when analyzing the yearly consumed electricity cost of the HP. These differences are shown in Figure 19. The larger savings are the ones seen in Albacete (4.7%), in which there are important heating and cooling demands throughout the whole year, as seen in Table 1. For the remaining cities, reductions of between 1.5% and 3.5% are observed.

Furthermore, the reduction seen in the absolute cost is also transferred to the specific cost. That is, when the controller is enabled, the system is able to provide heat at a lower price. These reductions can be seen in Figure 20. Comparing both the cost and the specific cost, the same trends can be derived: the larger reductions are obtained in Albacete (9.8%), while for the rest of the locations, reductions of between 3.8% and 7.8% are seen.
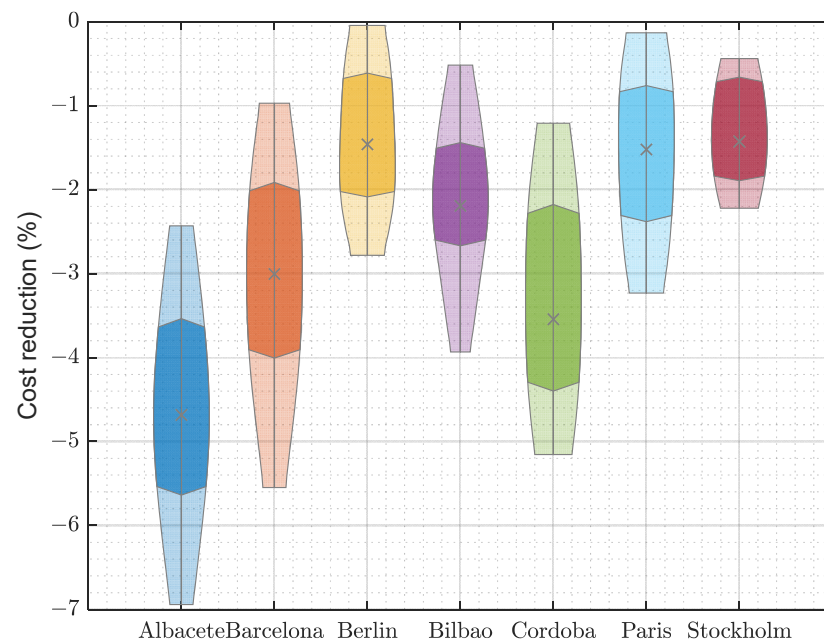
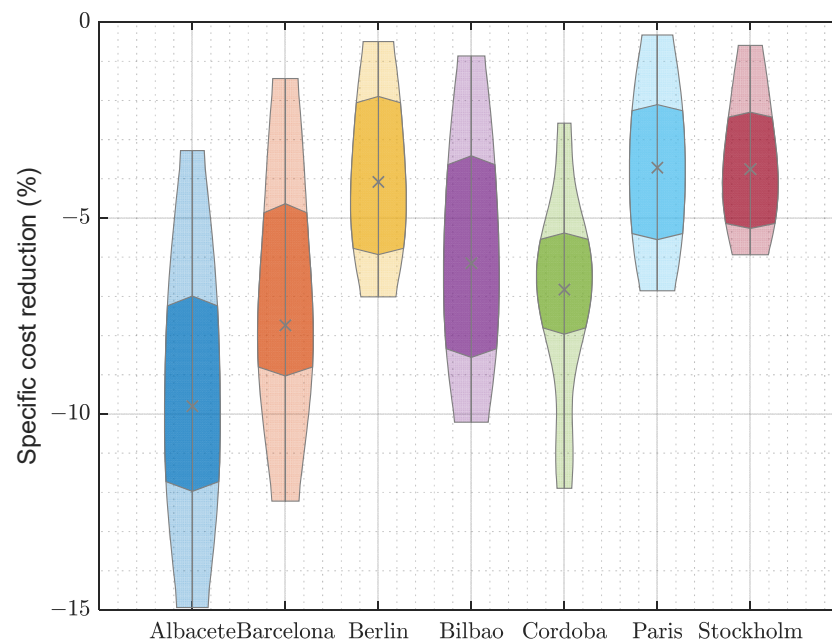**Figure 19.** Cost reduction for all climates.

Figure 20. Specific cost reduction for all climates.

Despite having a positive impact on both the self-consumption ratio and the cost, an effect that is often neglected when studying this kind of controller is the extra amount of both heat and electric power that is being consumed by the heat pump. These effects are shown in Figures 21 and 22, respectively. These increments of both the provided heat and the consumed power can be understood as a potential downside of this kind of controller, since it is a non-explicitly desired result (although the extra amounts of energy do not have a negative economic impact for the final user).
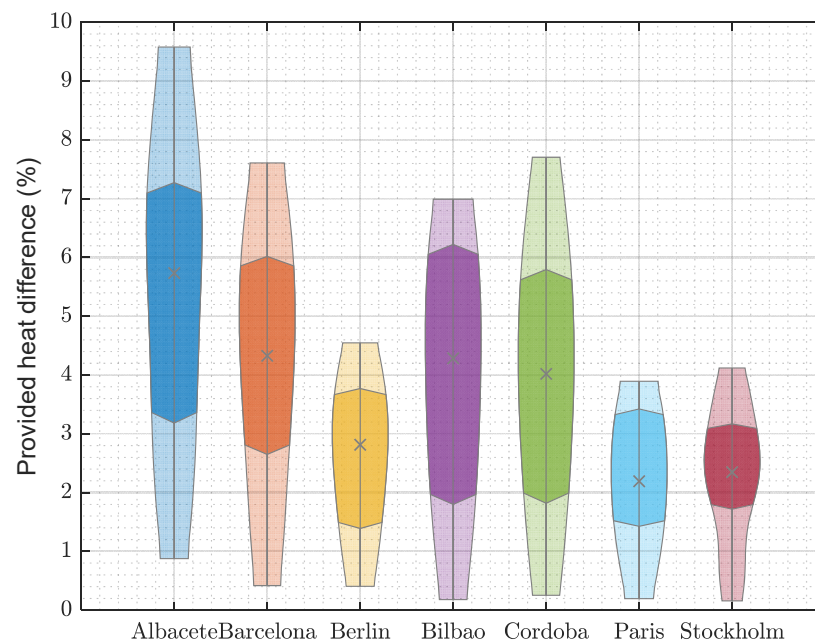
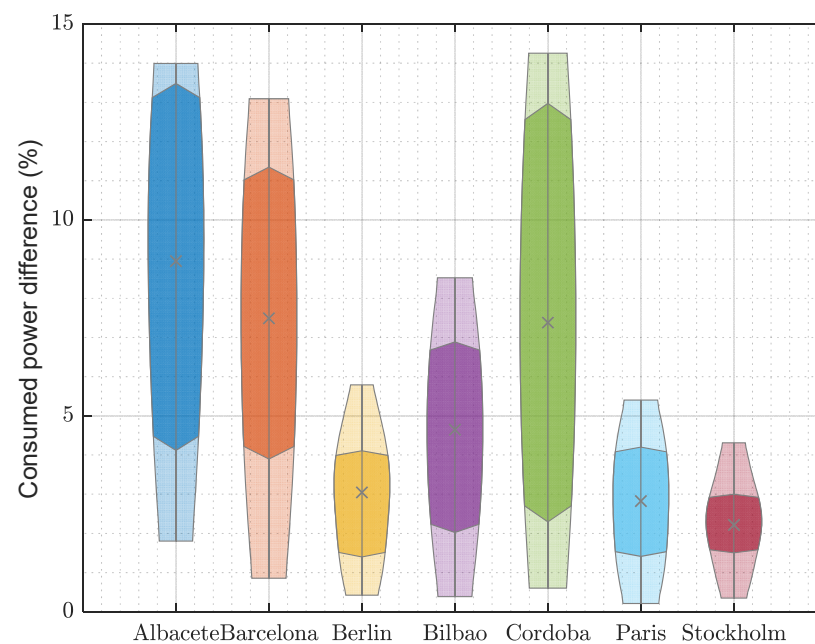**Figure 21.** Provided heat difference for all climates.

Figure 22. Consumed power difference for all climates.

Since the algorithm on which the controller is based aims to maximize the self-consumption, it turns on the heat pump when all the base demands are fulfilled. When that happens, new temperature set-points are applied: higher values for heating demands and lower values for cooling demands, which leads to more consumed power. Figure 23 shows how the cumulative distribution of the mean temperature in the condenser (understood as the arithmetical average between the input water temperature and the output water temperature) is different for the base case and the controlled scenario. When the controller is enabled, it is more common to have condenser temperatures of around 32–50 °C, caused by the new set-points of the space heating mode. The effect of the new temperature for the DHW is not that remarkable though, mainly because the activations of the heat pump in that mode are shorter and are not long enough to reach a steady-state situation.
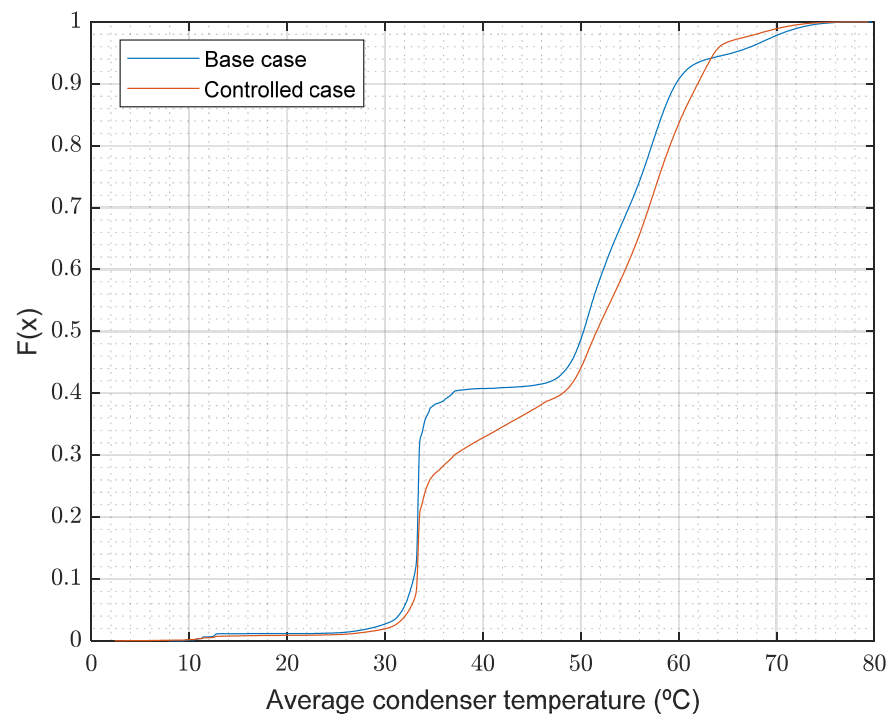
Figure 23. Cumulative distribution of the mean temperature in the condenser in heating mode for a specific case in Albacete.

The implemented algorithm not only changes the set-points of the tanks, but also the indoor temperature: fixing higher set-points in winter and lower ones in summer. The effect of changing these values is subjective and their potential impact on the comfort sensation may be hard to study numerically. Although it may be said that everything that deviates from the so-called standard set-points is a non-desired effect, the opposite might also be argued. That is, the user chooses more relaxed standard set-points in order to completely fulfill their comfort criteria only when the excess mode is enabled.

However, there will surely be a difference in the temperature distribution if the controller is activated. This effect can be seen in Figure 24 (for winter months) and Figure 25 (for summer months) for Albacete.

As can be observed, in Figure 24 (winter months), temperatures between 23 °C and 24 °C are more common when the controller is enabled. When compared to the base case scenario, the probability distribution seems to be moved 1 K to the right-hand side. On the other hand, in Figure 25 (summer months), it is clear how the temperature distribution is moved to lower temperature values.

In addition, once all the simulations were carried out, a regression analysis was carried out with two objectives. Firstly, to quantify the effect of each of the analyzed parameters on the final outcome in terms of self-consumption; and secondly, to derive a relatively straightforward equation that could be used to obtain an approximation of the operation of the system and the controller in other scenarios.
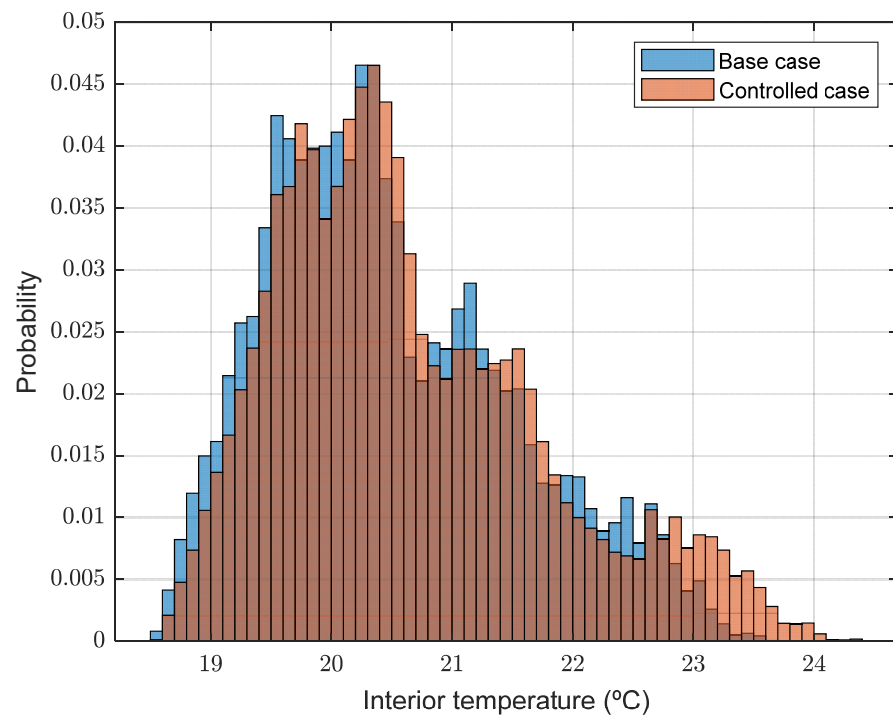
Figure 24. Probability distribution of the interior temperature in winter months for a specific case in Albacete.
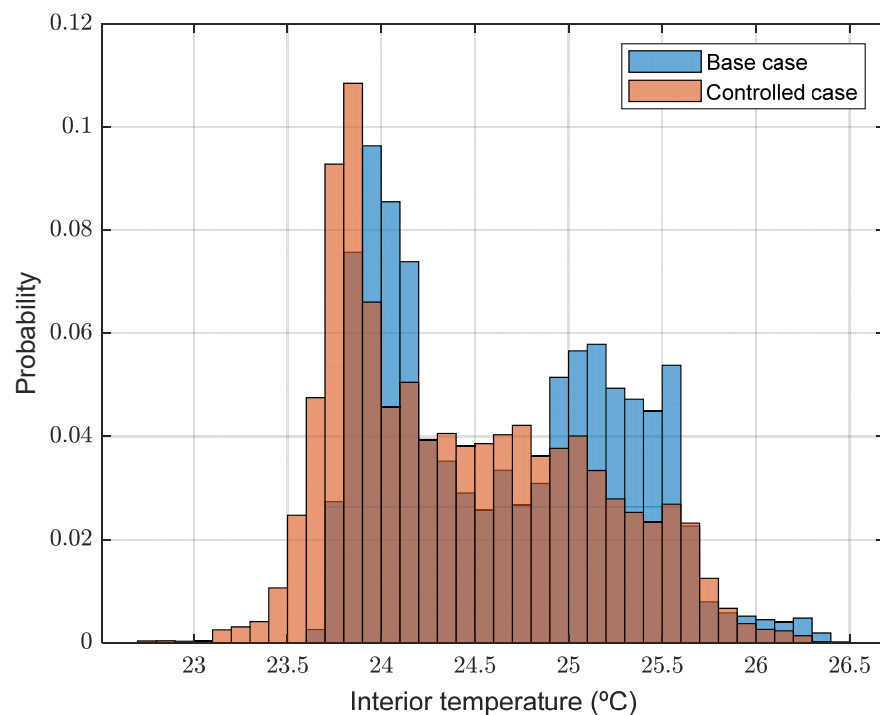

Figure 25. Probability distribution of the interior temperature in summer months for a specific case in Albacete.

Thus, the expression for the self-consumption ratio, shown in Equation (3), is proposed. Its inputs are the minimum photovoltaic excess to activate the excess mode ($PV_{min,excess}$), the yearly photovoltaic generation (E_{PV}), the yearly average temperature ($T_{year,ave}$), the yearly average horizontal solar irradiation ($H_{hor,year,ave}$), the heating demand per unit area (Q_{SH,m^2}), and the cooling demand per unit area (Q_{SC,m^2}).

$$SCR = a_0 + a_1 PV_{min,excess} + a_2 E_{PV} + a_3 T_{year,ave} + a_4 H_{hor,year,ave} + a_5 Q_{SH,m^2} + a_6 Q_{SC,m^2} \quad (3)$$

The derived coefficients can be seen in Table 5, while Figure 26 shows the comparison between the real and predicted values calculated by the linear regression. The dashed lines represent deviations of 8%. The model gives a root-mean-square error (RMSE) of 0.0189.

Table 5. Values of the coefficients for the linear regression.

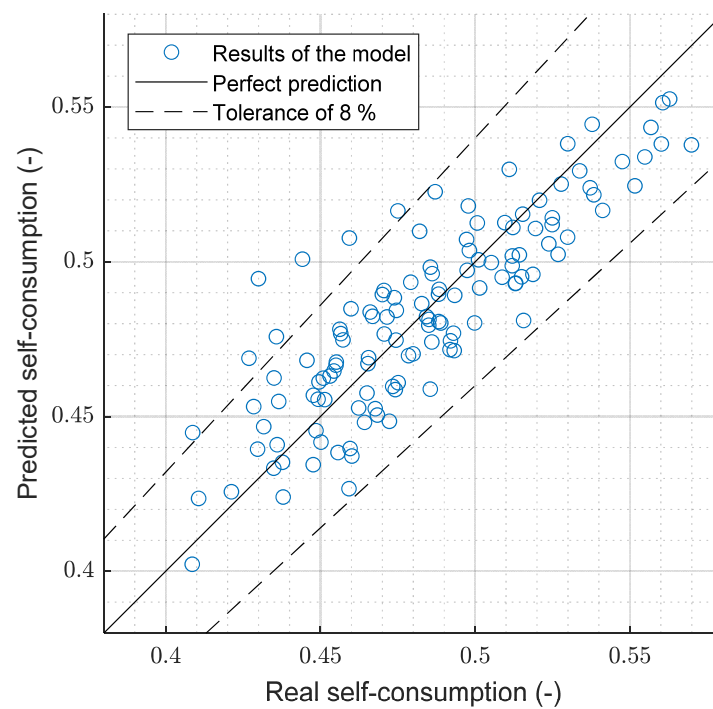| a0	-	0.505
a1	$PV_{min,excess}$	-0.000105
a2	E_{PV}	-2.69×10^{-5}
a3	$T_{year,ave}$	0.00435
a4	$H_{hor,year,ave}$	0.000546
a5	Q_{SH,m^2}	0.00116
a6	Q_{SC,m^2}	0.00141

Figure 26. Graph with the real and predicted self-consumption ratios by linear regression.

Nevertheless, the above equation is not useful for sorting out the impact of each of the variables, since it does not consider the range of the variables. Therefore, all variables have been normalized between 0 and 1, and the new coefficients are shown in Table 6 and Figure 27.

Table 6. Values of the coefficient for the normalized linear regression.

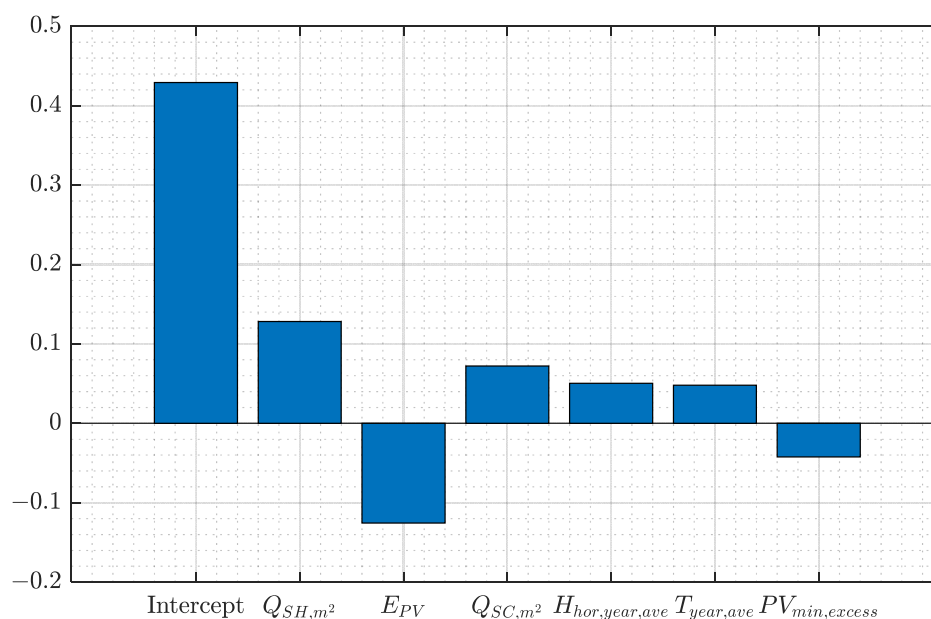| a0	-	0.429
a1	$PV_{min,excess}$	-0.0422
a2	E_{PV}	-0.125
a3	$T_{year,ave}$	0.0479
a4	$H_{hor,year,ave}$	0.0504
a5	Q_{SH,m^2}	0.1281
a6	Q_{SC,m^2}	0.0722

Figure 27. Bar diagram of the coefficients obtained in the normalized linear regression. The intercept corresponds to a_0.

From the analysis, it can be deduced that, within the cases that have been simulated, the most important variable when it comes to the self-consumption ratio obtained when the rule-based controller is enabled, is the heating demand per unit area. Considering only that variable, the higher the heating demand, the better the indicator will perform. This effect has been mentioned previously and is related to the fact that, in buildings with larger heating demands, the indoor temperature may go down during the central hours of the day. Thus, the controller has room to raise the temperature by switching on the heat pump and consuming the power that comes from the PV installation.

The total energy produced by the PV system has a similar coefficient, but with a negative sign. That is, the larger the PV generation, the smaller the self-consumption ratio will be. In systems where the PV installation is larger, not all the power coming from the panels can be consumed, not even when the controller is on.

In addition, the cooling demand per unit area comes with a positive sign, as do the mean irradiation and temperature. Finally, the minimum PV excess value to activate the excess mode is introduced with a negative impact. That is, with large values, the self-consumption goes down, but its impact is smaller than the heating demand, for example.

Furthermore, to deduce a more precise regression, interactions between variables have been introduced in the model. That is, with this approach, terms that consider the multiplication between variables are included: the result is an equation that contains 22 terms. By doing so, the model becomes more complicated, but it is able to better capture the performance of the self-consumption ratio. It has an RMSE of 0.0087. The results are shown in Figure 28, while the coefficients are set out in Table 7.
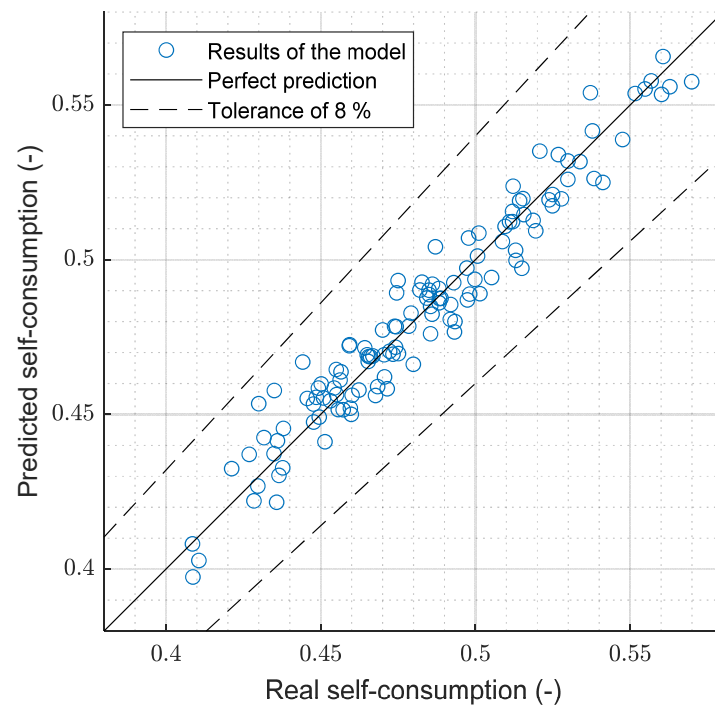
Figure 28. Graph with the real and predicted self-consumption ratios by linear regression considering interactions between variables.

Table 7. Values of the coefficient for the linear regression, considering interactions between variables.

a_0	-	0.338	a_{12}	$H_{hor,year,ave} : Q_{SC,m^2}$	0.0577
a_1	Q_{SC,m^2}	0.445	a_{13}	$Q_{SH,m^2} : Q_{SC,m^2}$	0.0490
a_2	E_{PV}	−0.287	a_{14}	$E_{PV} : Q_{SC,m^2}$	−0.0468
a_3	$T_{year,ave} : Q_{SC,m^2}$	−0.269	a_{15}	$PV_{min,excess}$	−0.0463
a_4	$E_{PV} : Q_{SH,m^2}$	0.253	a_{16}	$PV_{min,excess} : Q_{SH,m^2}$	−0.0288
a_5	Q_{SH,m^2}	0.209	a_{17}	$H_{hor,year,ave} : Q_{SH,m^2}$	0.0261
a_6	$T_{year,ave}$	0.162	a_{18}	$E_{PV} : H_{hor,year,ave}$	−0.0255
a_7	$T_{year,ave} : Q_{SH,m^2}$	−0.159	a_{19}	$PV_{min,excess} : Q_{SC,m^2}$	0.0102
a_8	$PV_{min,excess} : E_{PV}$	0.134	a_{20}	$PV_{min,excess} : T_{year,ave}$	0.00836
a_9	$E_{PV} : T_{year,ave}$	0.100	a_{21}	$H_{hor,year,ave}$	0.00274
a_{10}	$PV_{min,excess} : H_{hor,year,ave}$	−0.0899			
a_{11}	$T_{year,ave} : H_{hor,year,ave}$	−0.0596			

5. Conclusions

In this paper, a rule-based controller that aims to boost the self-consumption of a domestic combined PV-heat pump system is presented and analyzed.

The system (a household of 140 m^2 with a propane heat pump, two tanks and radiant floor) has been modeled according to CTE requirements and has been simulated using the Dymola and MATLAB-Simulink co-simulation feature. Heating and cooling demands are considered. Models used for the heat pump and the tanks have been calibrated and validated in laboratory tests.

The controller is based on a mode that is activated when there is enough PV excess to switch on the heat pump and all the standard demands are fulfilled. Once the mode has been activated, the set-points for the tanks and the indoor temperature of the building are raised (lowered when it works in cooling mode). Then, it measures the excess power that is

introduced in the electrical grid and tries to minimize it by modulating the compressor of the heat pump. Simple rules are proposed for controlling the compressor. If energy is being bought from the grid, or the base case set-points are not fulfilled any more, the controller deactivates the excess mode and the system works according to its standard working mode.

A parametric study with yearly simulations has been carried out to estimate the potential of the control strategy. Seven different European climates have been considered (with heating and cooling demands). In addition, two different insulation levels, three PV installation sizes and three minimum excess values for the excess mode activation have been analyzed. Improvements of up to 17% have been seen for the poorly insulated building in Stockholm for the self-consumption ratio. The greatest improvements can be observed when the insulation is low. Due to the fact that the indoor temperature goes down during the central hours of the day, there is a margin to activate the thermal inertia of the building. An improvement of 8–13% can be seen in the new building, whereas in the older building, the improvement is between 11% and 17%.

When translated to electricity cost, the largest reductions are obtained in Albacete (south-central Spain), which has both important heating and cooling demands. In this city, the average cost reduction is about 4.75%, while there are cases in which it is reduced by 7%. For the rest of the locations, the cost reductions are normally between 1.5% and 3.5%.

Nevertheless, due to the very nature of the controller, rises in both consumed power and provided heat can be seen when the new control is activated. In Albacete, there are cases in which the power consumed by the heat pump increases by 13%. For all climates, there are average increases of 2–9%. Although this extra energy comes directly from the PV installation, an increase in energy consumption is not something that is desirable when a controller such as this is implemented. In fact, it can be seen as a side effect that can overshadow the performance of the controller.

Furthermore, the potential of the controller is closely related to the increase (or decrease, in cooling mode) in the interior temperature set-point; and this decision could have a subjective nature. That is, for some users, increasing the set-point by a couple of degrees may cause a feeling of extra comfort or coziness; for others, it may be just the opposite, since they do not want a warmer temperature in their house. If the building is excluded from the control, the potential of the controller would decrease substantially, since the two tanks are relatively easy to charge.

Regarding the regression analysis, a simple linear expression has been elaborated to estimate the performance of the system if the controller is activated. It has been found that, within the range of the analyzed variables, the most important one is the heating demand. A larger heating demand means a larger potential of the controller. The same thing happens with cooling demands, but not as much. This can be explained by the activation of the heat pump in the central hours for cooling purposes. If, in the base scenario, the heat pump is activated in order to provide cold at midday, the controller has no margin to activate the excess mode. The sizing of the PV installation also has a great impact: the greater it is, the smaller the potential of the controller will be, since the excess power is directly introduced in the grid. Apart from the simple linear expression, a slightly more complicated equation with interactions between variables has been found with an RMSE of 0.0087; an expression that could be used to estimate the performance of the controller in other scenarios.

Author Contributions: Conceptualization, M.A.-L.; methodology, M.A.-L. and M.S.-M.; validation, M.A.-L.; writing—original draft preparation, M.A.-L.; writing—review and editing, M.S.-M., K.M.-E. and L.A.-O. All authors have read and agreed to the published version of the manuscript.

Abbreviations

Acronym	Definition
PV	Photovoltaic
COP	Coefficient Of Performance
DHW	Domestic Hot Water
MPC	Model Predictive Control
MPP	Maximum Power Point
CTE	Spanish Building Technical Code
NHH	New household
OHH	Older household
SH	Space heating
SC	Space cooling
RMSE	Root-mean-square error
HP	Heat pump
Variable	**Meaning**
T	Temperature
n	Rotational speed
w	Working mode of the heat pump (heat or cold)
SCR	Self-consumption ratio
$\dot{Q}$	Heat flow rate
$\dot{P}$	Consumed power
Subscript	**Meaning**
Comp	Compressor
Inner	Inner heat exchanger
Outer	Outer heat exchanger
Air	Ambient air
Water	Water through the heat pump
In	Input flow

References

1. European Heat Pump Association. Market Data-EHPA 2023. Available online: https://www.ehpa.org/market-data/ (accessed on 4 June 2021).
2. CAN Europe. Rooftop Solar PV Country Comparison Report-CAN Europe 2022. Available online: https://caneurope.org/rooftop-solar-pv-comparison-report/ (accessed on 24 May 2023).
3. Da Fonseca, A.L.A.; Chvatal, K.M.S.; Fernandes, R.A.S. Thermal comfort maintenance in demand response programs: A critical review. *Renew. Sustain. Energy Rev.* **2021**, *141*, 110847. [CrossRef]
4. Daikin. Daikin Altherma M HW 2022. Available online: https://www.daikin.eu/en_us/product-group/domestic-hot-water-heat-pump/daikin-altherma-m-hw2.html (accessed on 19 June 2023).
5. Ecoforest. Ecoforest se Adelanta a la ley de Autoconsumo Energético con su Gama de Gestores Energéticos 2019. Available online: https://ecoforest.com/es/blog/ecoforest-se-adelanta-a-la-ley-de-autoconsumo-energetico-con-su-gama-de-gestores-energeticos/ (accessed on 23 May 2023).
6. Vaillant. Energía Solar Fotovoltaica auroPOWER Energía Sostenible para Climatización y ACS 2023. Available online: https://www.vaillant.es/downloads/productos/auropower-1/auropower-catlogo-comercial-2061819.pdf (accessed on 19 June 2023).
7. Zanetti, E.; Aprile, M.; Kum, D.; Scoccia, R.; Motta, M. Energy saving potentials of a photovoltaic assisted heat pump for hybrid building heating system via optimal control. *J. Build. Eng.* **2020**, *27*, 100854. [CrossRef]
8. Péan, T.Q.; Salom, J.; Costa-Castelló, R. Review of control strategies for improving the energy flexibility provided by heat pump systems in buildings. *J. Process Control* **2019**, *74*, 35–49. [CrossRef]
9. Kuboth, S.; Heberle, F.; König-Haagen, A.; Brüggemann, D. Economic model predictive control of combined thermal and electric residential building energy systems. *Appl. Energy* **2019**, *240*, 372–385. [CrossRef]

10. Hazyuk, I.; Ghiaus, C.; Penhouet, D. Model Predictive Control of thermal comfort as a benchmark for controller performance. *Autom. Constr.* **2014**, *43*, 98–109. [CrossRef]

11. Fischer, D.; Madani, H. Smart Meter Enabled Control for Variable Speed Heat Pumps to Increase PV Self-Consumption Photovoltaics for Swedish Prosumers View project Ground Source Heat Pumps for Swedish multi-family houses: Innovative co-generation and thermal storage strategies Vi. In Proceedings of the 24th IIR International Congress of Refrigeration, Yokohama, Japan, 16–22 August 2015. [CrossRef]

12. Pinamonti, M.; Prada, A.; Baggio, P. Rule-based control strategy to increase photovoltaic self-consumption of a modulating heat pump using water storages and building mass activation. *Energies* **2020**, *13*, 6282. [CrossRef]

13. Psimopoulos, E.; Johari, F.; Bales, C.; Widén, J. Impact of boundary conditions on the performance enhancement of advanced control strategies for a residential building with a heat pump and PV system with energy storage. *Energies* **2020**, *13*, 1413. [CrossRef]

14. Fischer, D.; Bernhardt, J.; Madani, H.; Wittwer, C. Comparison of control approaches for variable speed air source heat pumps considering time variable electricity prices and PV. *Appl. Energy* **2017**, *204*, 93–105. [CrossRef]

15. Clauß, J.; Stinner, S.; Sartori, I.; Georges, L. Predictive rule-based control to activate the energy flexibility of Norwegian residential buildings: Case of an air-source heat pump and direct electric heating. *Appl. Energy* **2019**, *237*, 500–518. [CrossRef]

16. Domusa Teknik. Domusa Teknik 2023. Available online: https://www.domusateknik.com/es/portada (accessed on 20 June 2023).

17. Wetter, M.; Zuo, W.; Nouidui, T.S.; Pang, X. Modelica Buildings library. *J. Build. Perform. Simul.* **2014**, *7*, 253–270. [CrossRef]

18. Ministerio de Fomento. Documento Básico HE 2022. Available online: https://www.codigotecnico.org/pdf/Documentos/HE/DcmHE.pdf (accessed on 19 June 2023).

19. *UNE-EN 16147:2017*; Heat Pumps with Electrically Driven Compressors-Testing, Performance Rating and Requirements for Marking of Domestic Hot Water Units. AFEC: Madrid, Spain, 2017.

20. McKenna, E.; Thomson, M. High-resolution stochastic integrated thermal-electrical domestic demand model. *Appl. Energy* **2016**, *165*, 445–461. [CrossRef]

21. Jones, A.D.; Underwood, C.P. A thermal model for photovoltaic systems. *Fuel Energy Abstr.* **2002**, *43*, 199. [CrossRef]

22. ESIOS. ESIOS Electricidad 2023. Available online: https://www.esios.ree.es/es (accessed on 22 May 2023).

23. Clauß, J.; Georges, L. Model complexity of heat pump systems to investigate the building energy flexibility and guidelines for model implementation. *Appl. Energy* **2019**, *255*, 113847. [CrossRef]